Sphingolipid Gel/Fluid Phase Transition Measurement by Integrated Resonance Probe Light

Qingyue Li, Lucas Garnier, V. Vié, Hervé Lhermite, Alain Moréac, Denis Morineau, Claire Bourlieu-Lacanal, Aziz Ghoufi, Etienne Gaviot, Eric Gicquel, et al.

Sensors & Transducers, Vol. 225, Issue 9, September 2018, pp. 41-48

www.sensorsportal.com

Sensors & Transducers

Published by IFSA Publishing, S. L., 2018
http://www.sensorsportal.com

Sphingolipid Gel/Fluid Phase Transition Measurement by Integrated Resonance Probe Light

[1] Qingyue LI, [1] Lucas GARNIER, [1] Véronique VIE, [2] Hervé LHERMITE, [1] Alain MOREAC, [1] Denis MORINEAU, [3] Claire BOURLIEU-LACANAL, [1] Aziz GHOUFI, [4] Etienne GAVIOT, [1] Eric GICQUEL, [1, *] Bruno BÊCHE

[1] Univ, Rennes, CNRS, IPR (Institut de Physique de Rennes) - UMR 6251, F-35000 Rennes, France
[2] Univ, Rennes, CNRS, IETR (Institut d'Electronique et des Télécommunications de Rennes) - UMR 6164, F-35000 Rennes, France
[3] Univ Montpellier II, INRA CIRAD, IATE, F-334060 Montpellier, France
[4] Univ Maine, CNRS, ILAUM (Laboratoire d'Acoustique de l'Université du Maine) - UMR 6613, F-72000 Le Mans, France
Tel.: +33 (0)223235257
E-mail: bruno.beche@univ-rennes1.fr

Received: 25 June 2018 /Accepted: 31 August 2018 /Published: 30 September 2018

Abstract: The paper describes nanophotonic sensors realized by way of inexpensive organic processes. As hybrid silica/polymer resonators, they are suited to detect biological molecules in gel/fluid phase transition at infinitesimal concentrations (sphingomyelin lipids). Such a family of photonic structures is made of specific amplified deep UV210 photoresist-polymer waveguides coupled by a sub-wavelength gap with various racetrack micro-resonators. Thus, temperature dependent wavelength shifts characterizing the optical resonances of the device have been evaluated, highlighting a low thermal feature of the sensor, which is advantageous for this specific application. With an adapted vesicle lipid deposition process, specific in biology, together with an apt experimental thermo-photonic protocol, the dynamic evolution of the sphingomyelin lipid phase transition has been followed and assessed. The ability to detect their gel/fluid transition phase and melting temperature has been demonstrated with a mass product factor value 10^7 lower than that of classical methods as differential scanning calorimetry. The global equilibrium regimes of the coupling effect of resonances and the scattered part of the light are clearly highlighted as markedly modified by the dynamic of the sphingomyelin during its own phase transition.

Keywords: Nanophotonics, Microresonators, Sensors, Polymers, Lipids, Sphingomyelin, Phase transition detection.

1. Introduction

Microresonators [1] are useful components so as to shape and realize integrated photonic devices leading to the development of various applications: researches for engineering and optical telecommunications, biophysics, biochemical [2-3], biology [4] and biomedical. Such optical microcavities are interesting devices allowing to control optical fields as regards their spatial localization and lifetime $\tau=Q/\omega$, where Q represents the quality-factor of such an optical resonance and $\omega=2\pi\nu=2\pi c/\lambda$ are the pulsation, the frequency and the wavelength respectively. To a certain extent, as such resonant quantifications met in physics are due to a geometric recirculation of the light called whispering gallery modes (WGMs). These

quantifications emerge due to the installation of a cyclic condition (or stationary waves) written as $P_{opt}=t.\lambda_{Maxwell}$, with P_{opt} the 'optical'-perimeter of the microresonator and t an integer. This principle can be seen as the quantification of the orbital kinetic moment $\|\vec{L}\|=\|\vec{p}\wedge\vec{r}\|\equiv n.\hbar=\oint "mv".ds$ (as a quantified photonic orbital), where $\|\vec{p}\|=\hbar.\|\vec{k}\|=2\pi\hbar/\lambda_{Maxwell}$ quantity of movement, n integer, $r=P_{opt}/2\pi$ radius of the circle link to the previous P_{opt} perimeter, and $\hbar$ Planck or Dirac constant. Such WGMs modes increase both the field and merit of integrated photonics regarding a multiple set of optical telecommunications applications as components and transmissions (filters, modulators, de/multiplexing components, laser), together with sensors for metrology with platform analysis and detection procedure. The spatial localization of the light, due to the nature of the evanescent part of the light, acts as a tunable light probe for the surrounding so as to detect the changing environment. Various approaches and processes have been developed on different classes of materials in order to shape, on planar technologies (2D) or 3D-configurations, different shapes of microresonators (disk, ring, stadium, racetrack, sphere) [5]. Optical resonators based on organic materials exhibit a lot of advantages due to the well-established photolithographic technologies, the versatility of the polymer properties and functionalization and the possibility to be shaped starting from a liquid resist material with classical fluidic thin layer depositions. These controlled processes are reproducible concepts. The reasons of the progress in this research field are justified with the potential of numerous available materials, the simplicity of the relevant processes, the specific methods and measurements protocols. After the substantial development in optical telecommunications, organic materials based resonators have received intensive attention in metrology and sensing environmental applications, biology, medical and also food quality control. These photonics sensors relying on resonators have become the subject of research with important developments of sensing platforms devoted to the label-free detection of a variety of chemical, biochemical, biological agents and biomedical elements.

Sphingomyelin (SM) is a type of sphingolipid (or sphingophospholipids), found in animal and human cell membranes. SM is strongly prominent in myelin, a membranous sheath that surrounds and insulates the axons of numerous neurons. In animals and humans, SM represents 80 % of all sphingolipids, and typically make up 15 mol % in average of plasma membrane lipids; the higher concentrations are found in nerve tissues, gristles, blood cells and ocular areas… This plasma membrane component participates in many signaling pathways for electric information and transmission. The metabolism of SM creates many another products playing significant roles in the cell. The lipids used in such study is the sphingomyelin, which plays an important role in the particular function of plasma membrane of cells. This work is devoted to investigate low-cost reproducible polymeric photonic sensors integrated on a chip for such bio-detection. They are aimed to perform efficient sphingomyelin and lipid transition detection based on a gel-liquid state-change; this one corresponds to a melting temperature determination and then to a first order phase transition in biophysics.

2. Materials, Methods and Analyzes

Such section called Materials, Methods and Analyzes describes the global fabrication involving thin layer processes, starting from the chemical and materials aspects to achieve suitable deposition of biological samples, which are relevant in our compound approach. This comprises the use of attractive organic amplified photoresist with specific deep UV technology associated with an appropriate lipid deposition process related to biology. In addition, sundry characterization methods regarding the on-chip-device are described so as to validate both its concept and design. Furthermore, we also detail the versatile principle of operation and justify the measurements approach together with experiments developed for such a specific bio-metrology ascribed to temperature dependent lipid phase transition detection.

This transverse work features key points distributed over several levels considering: the nature of the specific organic with regard to materials, the technologies of thin layer processes for shaping the chips, associated with the method of deposition in biology (called fusion vesicle deposition method) and the whole protocol of measurements developed for such sensors: Then we highlight the ability to detect in a simple way any specific gel-liquid transition phase of sphingomyelin lipids with a mass product factor 10^7 lower than that of the conventional method called differential scanning calorimetry (DSC) that requires typically a quantity of substance averaging the mg. The first key point refers to the use of a polymer called UV210 from the photoresist chemistry (Shipley) based on deep UV processes and light/matter interactions [6]. We develop such a deep UV lithography approach at 248 nm (that is not the conventional peak, called i-line at 365 nm) by way of coupling a straightforward mercury lamp with an adequate and selective filter, as a significantly low cost method compared with electron beam lithography and ArF or KrF excimer laser or optical systems using F_2. Such an organic exposure to deep UV radiation at λ_{flash}=248 nm enables valuable low-cost realizations of sub-wavelength photonics structures considering the gap between waveguides and micro-resonators (MRs) within the order of λ_{flash} (due to the Raleigh's criteria and its associated spatial resolution limit). Such a deep UV (DUV) polymer made of poly p-hydroxystyrene and poly t-butyl acrylate is called an amplified chemical photoresist including a photo acid generator

(PAG) to increase the sensitivity with UV energy exposure as regards such a specific photolithography mechanism. Indeed the DUV-insolation induces the production with the PAG of a small quantity of acid acting as a catalyst during the exposure. Thermally activating this acid with a post exposure bake causes the proton H+ to act as a catalyst and unblock the group from the PHS. Then, the cascade of acid-activated chemical changes brings about a change in polarity of the polymer which goes from lipophilic to hydrophilic states. This make the PHS soluble in the exposed areas. Thus, DUV exposed areas become soluble in a basic developer as the tetra-methyl ammonium hydroxide. Relevant integrated DUV210 MRs photonics structures have been fabricated according to simple procedures and adequate parameters described in the next section.

2.1. Specific Materials Processes and Parameters to Obtain Sub-micrometer Resolution with Amplified Chemical Polymer (DUV210)

On a silicon substrate, a thermal silica layer is formed by wet oxidation method. We must first clean the wafer with the method RCA (developed by 'Radio Company of America'), to avoid all impurities. The plate is then put in a quartz oven with torch, the gas H_2 and oxidation gas O_2 being located in the flame for the combustion. A 3 hours stage in the oven at 1075°C can form 1000 nm of silica on the surface of the wafer, creating the silica lower cladding. After oxidation, the annealing at 700°C-800°C strengthens the single crystal structure. Such a thickness guarantees a highly stable and homogeneous refractive index under the organic waveguides and MRs so as to decrease the optical radiation losses regarding the propagation modes. After the substrate/cladding manufacturing, organic patterns are grown and shaped by way of specific processes involving deep UV lithography suited to the DUV210 polymer which is an amplified chemical resist. The adequate and optimized processes are illustrated in the following Table 1.

Table 1. Processes steps in cleanroom for UV210 polymer so as to shape MRs; (v, speed; a, acceleration; t, time; T, temperature; E, exposure dose).

Framework and Procedures (MRs in polymer)	**Parameters of the Steps** (v, a, t, T)
Spin-coating thickness, roughness	900 rpm, 5000 rpm/s, 30 s ~ 800-850 nm, ~ 2 nm
Softbake (t, T)	3min at 140°C
Deep UV (λ_{flash}=248 nm) exposure (OSRAM Hg lamp, dose, t)	E=20 mJ/cm^2, 27 s
Post-exposure softbake (t, T)	1 min at 120°C
Development (t, product)	30 s, Microposit MF CD-26
Final softbake (t, T)	12 h at 120 °C

A baking step makes the surplus solvent to evaporate and strengthens the adhesion of the polymer onto silica. The deep UV exposure is performed with a mercury short arc lamp (HBO 1000W/D, OSRAM). A quartz chromium mask is arranged above the wafer with the spread polymer layer. The lithographic pattern to be transferred is printed onto the mask and a 27 seconds exposure duplicates the mask patterns on the wafer in a suitable way. A 1 min annealing at 120 °C promotes the polymerization reaction so as to minimize the surface roughness (< 3 nm). Then, immersion in the developer Microposit MF CD-26 allows us to get the whole chip featuring the MRs. In order to optimize the test and the adequate photonic injection, integrated chips on such DUV210/SiO2/Si multilayers are cleanly cleaved by way of a diamond tip. As an example, Fig. 1 illustrates the scanning electron microscopy (SEM) image of a typical 2 µm-width rib waveguide (after the processes previously described in Table 1). So as to maintain single-modes operations, the height is shape close to the wavelength value that is close to 900 nm.

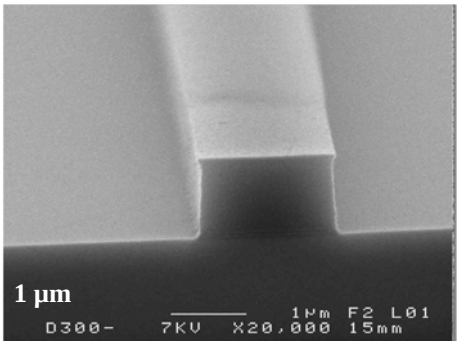

Fig. 1. Scanning electron microscopy (SEM) image; perfect aspect of the injection face.

Such an approach contributes to a valuable repeatability for mass production of cleanable and re-usable sensors. So as to operate on quasi-TE_{00} and -TM_{00} single-mode eigenvectors, adequate and straightforward simulations have been previously achieved considering the theory of electromagnetism in waveguides allowing us to obtain eigenvalues equations: then, all the series of quantified effective propagation constants $\beta=k_0.n_{eff}$ or effective indices n_{eff} can be settled defining then the apt opto-geometric parameters for such photonic structures as explained in next section.

2.2. Theory on Optic and Geometric Considerations Concerning the TE_{00}-TM_{00} Single-mode Behavior

These typical dimensions (h-height and w-width) regarding refractive indices enable us to operate with exclusive optical single-mode TE_{00}-TM_{00}. The methodology supporting such simulations consists in

solving the J.C. Maxwell's equations in each part of the whole system while taking into account the continuity properties of the electromagnetic fields so as to obtain the so-called eigenvalues equations that highlight directly the overall quantifications of the fields viewed as eigenvectors. Such photonic structures or opto-geometrical systems show-off an intrinsic asymmetry especially in the optical indices entailing a cut to occur in the dispersion curves of the modes. As an example, considering the first operation of quantification along the direction perpendicular to the wafer surface with regard to the apt electromagnetism theory, it is easy to define the cut-thickness notion regarding both the TE_m and TM_m modes (m integer) within our structure:

$$h_{cut} = \frac{\lambda_0}{2\pi\left(n_{DUV210}^2 - n_{SiO2}^2\right)^{1/2}} \{arctg[\Phi] + m\pi\}, \quad (1)$$

where

$$\Phi = \eta_{DUV210/upper-cladd}\left(\frac{n_{SiO2}^2 - n_{upper-cladd}^2}{n_{DUV210}^2 - n_{SiO2}^2}\right)^{1/2}$$

Here, $n_{material}$ stands for the relevant refractive indices, considering the DUV210 polymer core and respective claddings (lower SiO_2, upper air or lipids) at $\lambda_{0\text{-wavelength}}$; also, $\eta_{DUV210/upper-cladd}$ = 1 or $\left(\frac{n_{DUV210}}{n_{upper-cladd}}\right)^2$ for their respective TE_m and TM_m polarizations.

The h_c cut-thickness values for TE and TM polarizations are respectively equal to 195 nm and 256 nm (for *m*=0), plus 800 nm and 860 nm (for *m*=1). Below the h_c-values at *m*=0, with no eigenvectors TE_0 and TM_0 allowing the light to occur, a consequent forbidden area is located out of the cone of light; the latter gives rise to the dispersion curves related with the family of bounded or guided modes. Between the ranging of h_c-values corresponding to the cut-thicknesses at respectively [m=0; m=1], both TE_0- and TM_0 single-modes occur and propagate with a high probability of presence. A rib waveguide typically 800 nm in thickness × 2 µm DUV210, arranged onto SiO_2/Si makes certain to maintain a single-mode characteristic: then, the device may be operated with respectively the optical propagation, an apt optical coupling between the waveguide and the micro-resonator element featuring the optical resonance phenomenon.

2.3. Analyzes of Materials and Quality of the Photonic Structures

Strict quality controls of the chip (materials, properties, geometries, sub-micron dimensions, surface aspects and so on) are then necessary with the help of various technologies and instrumentations concerning imaging and analysis: optical microscopy that may involve imaging with Nomarski operation in Differential Interference Contrast (DIC), Atomic Force Microscopy (AFM, BRUCKER Nanoscope 8), Scanning Electron Microscopy (SEM) and Raman micro-spectroscopy and imaging (Fig. 2).

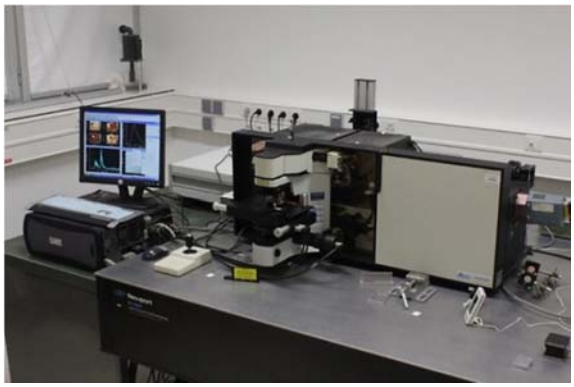

Fig. 2. Photograph of the whole Raman platform analysis.

The LabRAM HR800 Raman Spectrometer (from Horiba Scientific company, Jobin-Yvon) is a high-resolution spectral spectrometer coupled with a confocal microscope, several laser sources (633 nm He-Ne), (785 nm Toptica) and (532 nm Coherent) and nano-positioners. The coupling with a confocal microscope enables us to imaging a sample in 2D with a spatial resolution of the order of the spot size (0.9 µm) in the focal plane and a spectral resolution of typically 1 cm^{-1} per pixel. An apt laser excitation power lower than 0.1 mW is devoid of heating effect onto the photonics chip. Due to the 2D-planar geometry of the sensor, Raman spectroscopy is performed assuming a two dimensional analysis. Top view photographs by optical imaging and AFM allow to measure either globally or specifically located in specific areas, various geometric parameters regarding the waveguide/racetrack MRs devices (Fig. 3).

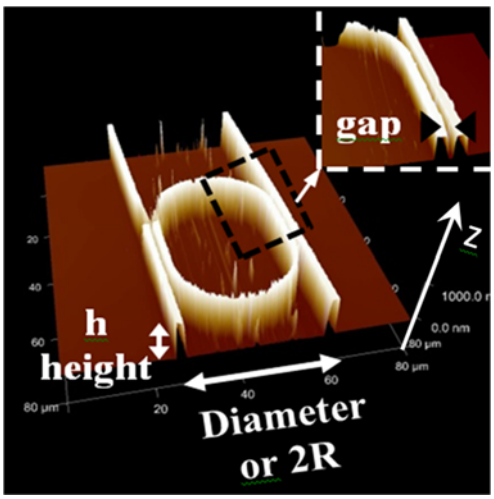

Fig. 3. AFM imaging: control of the photonic device including waveguide coupled with racetrack-resonator: with g-gap, h-height and R-radius of circle part.

The images were acquired in tapping mode in air. The z-scale is 1µm and the image size is (80×80) µm². Then, may be assessed: the *g*-gap of the evanescent physics of the coupling or the optical tunnel effect equal to 540 nm (for an interesting selectivity), the coupling length (L_c=15µm) allowing to the light the time both to transit and couple into the resonant part of the MR circuit, plus the respective dimensions of radius R=15 µm, w=2 µm and h=860 nm allowing only the single-mode existence of mathematic eigenvectors (TE_{00} and TM_{00}) considered with a λ_0=795 nm propagation wavelength (or laser).

Moreover, the DUV 210 surface analysis with AFM has confirmed a roughness lower than 2 nm clearly minimizing the optical losses due to parasitic diffraction. The photonic structure was imaged with the MultiMode 8, an atomic force microscope from Brucker.

The studies by micro-Raman vibrational molecular spectroscopy and analysis measurements without destruction of materials, were carried out and results recorded on a LabRAM HR 800 used in visible configuration (Fig. 2). The micro-Raman spectroscopy analyses and detection of various signal signatures of each micro-material, can be led and the specific complex signal of the organic DUV210 established (stretching mode of phenyl ring at 1002 cm^{-1} and the bending mode of aromatic olefinic at 855 cm^{-1}, Fig. 4). Moreover, filtering the enlarged signature and then choosing specific peaks characterizing the DUV210 (for example at 1002 cm^{-1}) it is also possible to image on 2D the waveguide/MR structure for a stringent quality control on geometry and materials.

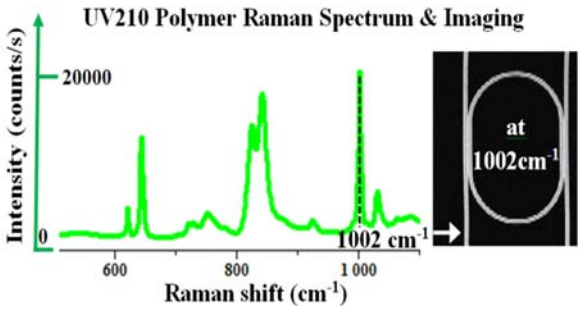

Fig. 4. Raman spectroscopy analyses of UV210 polymer plus Raman top view imaging of the overall photonic device by choising 1002 cm^{-1}.

Concerning the lipid substance and deposition, Fig. 5 represents the chemical structure of the sphingomyelin which has been deposited by vesicle fusion method.

Milk sphingomyelin (MSM) was purchased from Avanti Polar Lipids (Alabaster, AL, U.S.A.) under lyophilized powder form with the purity of 99 % [7]. After solubilization in chloroform/methanol (1:2, wt), the solvent is removed under nitrogen flux. Then, the lipid film was solubilized in Milli-Q water at the final concentration of 1 mg/mL. This aqueous solution was sonicated until it appears clear in order to form a suspension of small unilamellar vesicles. The temperature was maintained over 50 °C to keep the lipid in fluid phase. Typically a droplet of 3 µL of the lipid solution was deposited on the top of the device. The sedimentation and vesicle fusion lead to a multilayer formation on the top of the device. Then, a very low flux was applied to evaporate the water. The surface covered with the lipid film is around 5.5 mm². The thinness was then estimated at 300 layers of lipids that is typically 750 nm of lipids (Fig. 6).

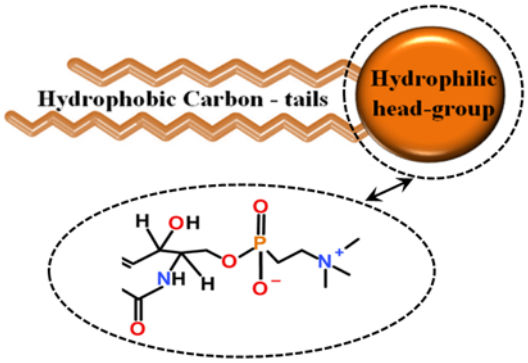

Fig. 5. Sphingomyelin: symbolic representation.

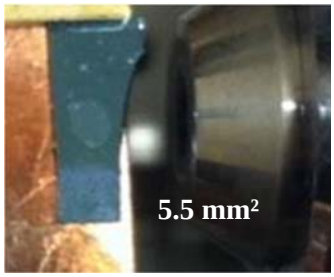

Fig. 6. Sphingomyelin after vesicle fusion deposition onto photonics MRs-structures; photography as upper-view.

Such a previous measurement is based on the calculation of the number of lipid molecules deposited (in 3 µL) with respect to the number of molecules necessary to cover the surface stain. Thanks to compression isotherms performed on the Langmuir trough, the mean molecular area of lipids can be determined and for MSM, this value is around 70 Å². The number of molecules necessary to cover homogeneously the stain of 5.5 mm² with a single layer is 7.86×10^{12} molecules. In the other hand, the volume deposited on the surface is 3 µL of a solution at 1 mg/mL (amounting to 3 µg deposited): then, knowing the molar weight of MSM (MM_{MSM}=801.22 g/mol) and with $N_A=6.022\times10^{23}$ /mol the Avogadro number, the number of molecules deposited is $(3\times10^{-6}/MM_{MSM}\times N_A)=2.25\times10^{15}$, inducing the arrangement of about 300 lipid layers

($2.25\times10^{15}/7.86\times10^{12}$=287). The thickness of bilayers being usually given around 5 nm, then one layer is estimated about 2.5 nm in thickness. Hence, considering all of these parameters, the estimated thickness of the film averages 750 nm. The AFM analyzes also make possible to obtain the roughness profile of the deposited myelin (Fig. 7).

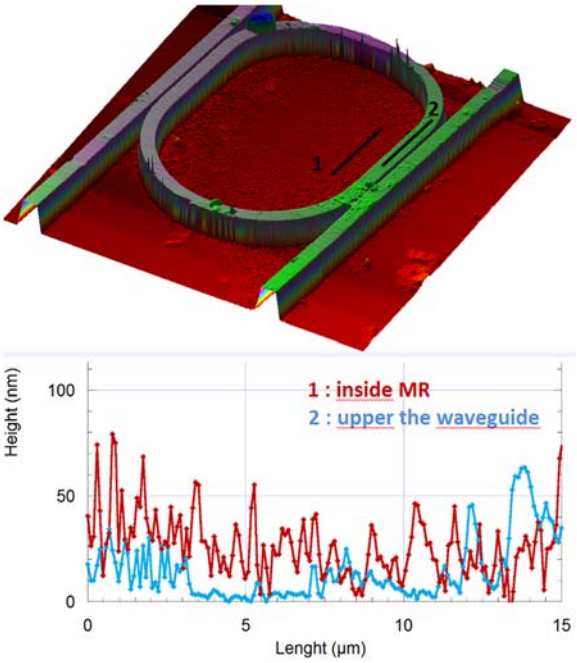

Fig. 7. AFM imaging after sphingomyelin deposition and drying at room temperature.

The synoptic of the method with the experimental protocol and principles of measurements (with or without previous lipid deposition) starting from the photonic platform arrangement devoted to optical preparation mode, injection and operation control, until the methodology of dynamic spectral measurements and statistical treatments in time so as to detect such lipid phase transition precisely.

2.4. Differential Scanning Calorimetry (DSC), Lipid 'gel ⇔ fluid' Phase Transition Detection

The melting behavior of the sphingomyelin was monitored using differential scanning calorimetry (DSC) (DSC Q20; TA Instruments, Guyancourt, France). 2 mg of dry lipids were loaded into the DSC sample pan and hydrated with Milli Q water to reach the final concentration of 20 % wt sphingomyelin. The pan was sealed. An empty, hermetically sealed, aluminum pan was used as reference. The calorimeter was calibrated with indium (5.1 mg, ΔH= 31.24 J/g, melting point = 156.48 °C), assessing the accuracy of the temperature measurement to +/-0.1°C and +/-10 % for the heat flow. The lipid sample was first heated up to 70 °C then cooled down to 10 °C and finally heated up to 70 °C. The melting temperature of milk sphingomyelin associated to the transition from the gel phase to the fluid phase was determined from the onset point: that is the intersection between the baseline and the line tangent to the main peak. The transition was found at T_m=31 °C in the heating thermogram recorded at 5 °C/min (blue, Fig. 8). In the same manner we can measure such a transition from the fluid phase to the gel phase (red, Fig. 8).

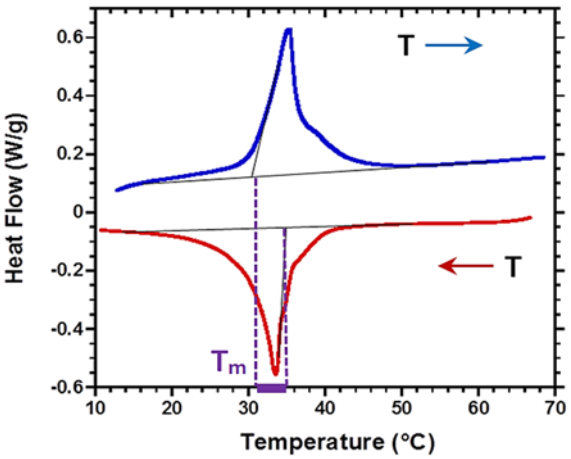

Fig. 8. DSC experiments on milk sphingomyelin: thermogram (endothermic heat flow up or exothermic heat flow down) and determination of the T_m.

Three scanning rates (0.5, 5 and 10 °C/min) were used to assess hypothetical kinetic effects on the shape of the thermogram. It confirmed that the T_m is not affected by the scanning rate, and that the shoulder actually reflects thermodynamical features of the phase transition and not kinetic distortions. Finally, the calorimetric results are in accordance with the literature. The lower value of the melting temperature (from the gel phase to the fluid phase) was evaluated at T_m=31 °C; this value depends to the differences in the sample composition. The presence of ions in the solvent could displace the phase transition by changing the head-group packing which adds lateral strain shifting the T_m up to high values. In contrast with pure molecule phase transition, the thermogram showed a broad peak, the phase transition occurs on a temperature range of several degrees. This effect is related to the length heterogeneity of the hydrocarbon chains. Milk SM present long chains containing 20 until 24 carbons. Comparing the T_m value with sphingomyelin obtained from the other sources such as egg or brain, T_m of milk sphingomyelin is lower due to the presence of more unsaturation hydrocarbon chains (saturated / unsaturated ratio is close to 30 %).

In such DSC analyses, the usual required concentration to detect the temperature of the lipid transition is 10 mg with a solution at 20 % (W/W) of lipid yielding then 2 mg of lipids. In our case, with said photonics sensor, we used one drop of a 3 µL solution at 1 mg/mL, entailing 3 µg deposited on the chip

which contains the resonators as explained previously. However, we have to take into account the surface of the micro-resonator (MR) which is the probe, because it comes up as a significant interaction light/lipids matter. The resonant light contributing to the principle of measurement is only located into the MR. Its active surface is (125×2)=250 μm² as depicted in Fig. 3 with 125 μm as the round (or length) of the racetrack-MR and 2 μm the width of the rib waveguide. Then, for the abovementioned 750 nm-thickness on top of this active-MR surface (with 250 μm^2 being 22000 times less than the initial 5.5 mm^2), the number of molecules to be considered as interacting with the light is then 1.07×10^{11}, ($\times N_A$) or 1.78×10^{-13} mol, ($\times MM_{MSM}$) or 1.426×10^{-10} g of MSM lipids. Then in comparison to the previous quantity, 2 mg of lipids used in the DSC method, we have used 1.4×10^7 (more than 10 millions) less product in interaction with the light in such a principle hinging on MR measurement as explained next.

3. Optical Resonance Measurements, Sensor Detections and Discussions

In this section called Optical resonance measurements, Sensors detections and Discussions, the significant low-thermal feature of the chip device (sensors without lipid deposit) is clearly established: the system is low-sensitive to temperature changes in a wide range from 16 °C to 42 °C. Such a feature is most appropriate to detect specific molecules localized on the top of the chip so as to assess their relevant biomechanisms. The ability to follow the dynamic evolution of sphingomyelin with temperature by detecting their own gel/fluid transition phase can be emphasized, together with the determination of the melting temperature due to changes of the specific parameters of the optical spectra.

Our sensors are based on a coupling and resonance physics, with a tunnel effect through a gap added with an optical geometric and cyclic resonance (Fig. 7 and Fig. 9). Fig. 9 represents the schematic photonic chip under test, allowing adequate coupling from the waveguide to the resonators and the apt circulation into the racetrack loop so as to probe the MSM phase transition.

A broadband source is used to highlight and create relevant quantified resonant modes. A single mode fiber is connected to the laser source (SUPERLUM, SLD 331 HP3) and a lens system is arranged to focus the incident beam and achieve this type of photonic micro-nano-injection. A polarizer and a (λ/2)-blade secure the polarization state, TE or TM. The sample holder is connected to a temperature controller (Peltier type plus thermoelectric temperature controller ILX Lightwave LDC3900) with which one can control the real-time experience temperature, allowing the thermal stability of the optical sensors to be validated. The supports are controlled with nano-piezoelectric actuators (PI-563I.3 E) with a ± 10 nm pitch in the three spatial dimensions. Such handlings and other specific injection protocols are used to excite and measure the quantified resonances. A third lens is positioned to recover the output light; then, a splitter cube distributes 30 % of the output power to a CCD camera (Pulnix CCD imaging so as to monitor and control the single-mode video characteristic), while the other 70 % of the signal is collected with a second single-mode fiber to be sent to the Spectrum Analyzer Optical (OSA Ando AQ-6315E or OSA Anritsu MS9710C).

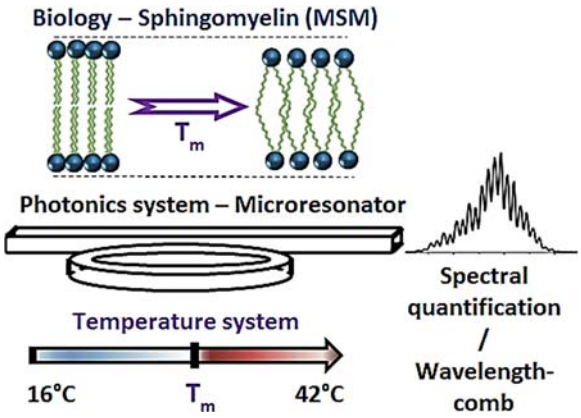

Fig. 9. Schematic principle of the photonic and lipid 'gel/fluid' phase transition detection. Thermal and mechanical systems controls, computing and signal processing have been installed and implemented.

Our protocol is then to record resonant a serial of spectra at fixed temperature by the photonic device and quantification probe light with OSA and relevant computer treatment, with λ_i (i, integer) the peaks wavelengths, Δλ and δλ parameters respectively associated with the resonant wavelengths, the Free Spectral Range (Δλ–FSR) and the Full Width Half maximum (δλ–FWHM). The Δλ–FSR can also be determined in parallel with a Fast Fourier Transform calculus on the comb-shaped periodic wavelength allowing then its quantification.

Considering the electromagnetic set of equations describing our design, the operating regimes specifying the quantified values of the coupling factor κ from the guide to the resonator are justified. Indeed, the optical transmission of such devices depends on intrinsic parameters, namely κ the coupling factor, the intra-cavity losses, the absorption plus the roughness. [8]. The equilibrium of the regime is clearly broken by the dynamic of the MSM and its own phase transition (Fig. 10).

The ability to detect the specific gel/fluid transition phase of MSM lipid and the efficiency to pinpoint the melting temperature at T_m = 31± 0.5°C have been demonstrated. Moreover, differential scanning calorimetry thermograms and their related analysis measurements corroborated exactly the results stemming from our light-sensors (Fig. 8).

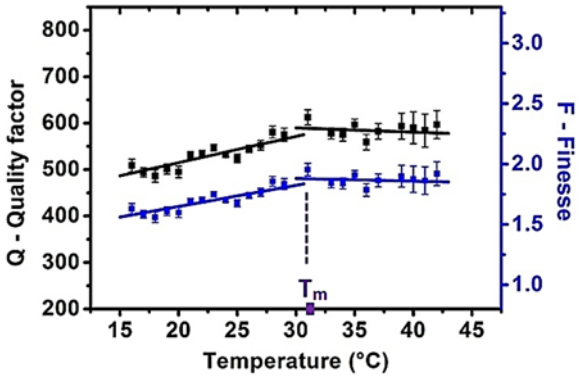

Fig. 10. Quality Detection of the gel-liquid phase transition of SPH lipids. Evolution in temperature of the quality factor $Q=\lambda_0/\delta\lambda$ and Finesse $F=\Delta\lambda/\delta\lambda$ of the photonic device under lipid test (MSM), determination of $T_m \approx [31\text{-}32]$ °C.

4. Conclusions

In conclusion, the dynamic evolution of the milk sphingomyelin (MSM) lipid phase transition was assessed by relevant photonics MRs sensors: the ability to detect their own gel/fluid transition phase and T_m melting temperature has been demonstrated: the balanced regimes of the resonators were clearly observed as markedly broken by the dynamic of the sphingomyelin and their specific phase transition prior relevant detection.

Acknowledgements

The authors would like to thank the 'Direction de l'Innovation et des Relations avec les Entreprises' (DIRE) of the CNRS plus Rennes Metropolis for financially supporting this research.

References

[1]. D. G. Rabus, Integrated ring resonators: The Compendium, *Springer Verlag: Berlin Heidelberg New-York*, 2007.

[2]. C. Ciminelli, C. M. Campanella, F. Dell'Olio, C. E. Campanella, M. N. Armenise, Label-free optical resonant sensors for biochemical applications, *Progress in Quantum Electronics*, Vol. 37, Issue 2, 2013, pp. 51-107.

[3]. R. Castro-Beltran, N. Huby, V. Vié, H. Lhermite, L. Camberlein, E. Gaviot, B. Bêche, A laterally coupled UV210 polymer racetrack micro-resonator for thermal tunability and glucose sensing capability, *Advanced Device Materials*, Vol. 1, Issue 3, 2015, pp. 80-87.

[4]. B. Bêche, Q. Li, V. Vié, L. Garnier, H. Lhermite, C. Bourlieu-Lacanal, E. Gaviot, A. Moréac, D. Morineau, A. Ghoufi, D. Dupont, E. Gaviot, Investigating the detection of lipids gel/fluid phase transition by change of scattering light and coupling factor into optical microresonators, in *Proceedings of the 1st International Conference on Optics, Photonics and Lasers (OPAL'2018),* Barcelona, Spain, 9-11 May 2018, pp. 10-12.

[5]. R. Castro-Beltran, N. Huby, G. Loas, H. Lhermite, D. Pluchon, B. Bêche, Improvement of efficient coupling and optical resonances by using taper-waveguides coupled to cascade of UV210 polymer micro-resonators, *Journal of Micromechanics and Microengineering,* Vol. 24, 2014, pp. 125006.1 – 125006.7.

[6]. Shipley UV210 web site, (http://micromaterialstech.com/products/duv-photoresist-dow-rohm-and-haas/dow-uv210-photoresist/).

[7]. Avanti polar web site, (https://avantilipids.com/product/860063/)

[8]. N. Michel, A.S. Fabiano, A. Polidori, R. Jack, B. Pucci, Determination of phase transition temperatures of lipids by light scaterring, *Chemistry and Physics of Lipids*, Vol. 139, Issue 1, 2006, pp. 11-19.